

Division - Soil Processes and Properties | Commission - Soil Physics

Cracking process in expansive soil with and without vegetation covers in dry and rainy seasons at field scale

Silvio Romero de Melo Ferreira^{(1)*} , **Arthur Gomes Dantas Araújo^(1,2)**  and **Martha Maria Bezerra Santos⁽¹⁾** 

⁽¹⁾ Universidade Federal de Pernambuco, Departamento de Engenharia Civil e Ambiental, Programa de Pós-Graduação em Engenharia Civil, Recife, Pernambuco, Brasil.

⁽²⁾ Universidade Federal Rural Semi-Árido, Departamento de Engenharias, Angicos, Rio Grande do Norte, Brasil.

ABSTRACT: The presence of desiccation cracks in the soil alters its hydromechanical behavior, increasing the soil's water infiltration capacity, mobilizing the potential for expansion. This may affect the performance of the structural elements of the construction. This study aimed to evaluate the mechanics of expansion, contraction and cracking of the expansive soil of Paulista - Pernambuco, Brazil, through field trials, subject to wetting cycles and drying. The studied soil is a sandy silty clay of high compressibility with medium to very high expansion potential. The process of formation and propagation of cracks was analyzed using digital images and the monitoring of samples subjected to drying and wetting cycles. The indices of crack geometry increased with the advancement of desiccation but did not stabilize. During the wetting period, they tend to close. The pattern of cracks in the tests varied according to the presence or absence of vegetation. It was concluded that the vegetation cover has a significant influence on the standardization and the crack formation and propagation process.

Keywords: expansive clay, vegetation, expansion, contraction, wetting and drying cycles.

* **Corresponding author:**
E-mail: sr.mf@hotmail.com

Received: May 20, 2023

Approved: July 05, 2023

How to cite: Ferreira SRM, Araújo AGD, Santos MMB. Cracking process in expansive soil with and without vegetation covers in dry and rainy seasons at field scale. Rev Bras Cienc Solo. 2023;47:e0230055
<https://doi.org/10.36783/18069657rbc20230055>

Editors: José Miguel Reichert  and João Tavares Filho .

Copyright: This is an open-access article distributed under the terms of the Creative Commons Attribution License, which permits unrestricted use, distribution, and reproduction in any medium, provided that the original author and source are credited.



INTRODUCTION

Expansive soils are problematic for buildings and infrastructure worldwide, causing socioeconomic and environmental damage due to volumetric variations when suffering moisture variation. Two main requirements are needed for soil to display expansiveness. An intrinsic factor related to the soil mineralogical composition, texture and structure, and an extrinsic factor that is capable of transferring moisture from one point of the soil to another, related to climatology, hydrogeology, vegetation, and occupation capacity (Chen, 1988; Ferreira, 1995; Nelson et al., 2015).

They are often identified in arid or semi-arid regions where evapotranspiration exceeds volumetric precipitation. Expansive soils increase in volume when flooded and decrease in volume with water evaporation. Climatological conditions affect soil moisture, increasing or decreasing volume (Ferreira, 1995; Guerreiro et al., 2021).

Studies were carried out to evaluate the influence of the surroundings on soil moisture, such as the influence of air humidity, vegetation, and rainy seasons. Seasonal variations in the environment subject the soil to alternating dry and wet periods. It has already been observed that in a dry period longer than 30 days, micro-cracks open in the soil (Guerreiro et al., 2021, 2022). During dry periods, the soil retracts and forms cracks that propagate, altering its mechanical and hydraulic properties. Hydraulic conductivity increases due to the formation of cracks, generating a quick and direct movement of water and solutes from the soil surface to the permeable substrate, and in compacted landfills, the crack reduces resistance, generating infiltration and percolation problems (Chen, 1988; Fredlund and Rahardjo, 1993; Ferreira and Ferreira, 2009).

As mentioned, in addition to the climatological factor, the volume of water in the soil is also influenced by vegetation, which extracts water and dissolved minerals through its roots. Thus, vegetation reduces the saturated permeability and increases the air-entry suction of soils. However, roots in the soil generate greater tensile strength, which tends to suppress cracks and swelling (Jotisankasa and Sirirattanachat, 2017; Ferreira et al., 2020).

Hence, there are five main points to be discussed about soil desiccation cracking in vegetated soil. First, transpiration-induced soil suction increases tensile stress along the crack plane. Second, root reinforcement resists soil deformation. Third, the effects of plant root exudates on altering soil aggregation. Fourth, the influence of tree spacing and plantation practices on crack initiation. At last, plant traits such as stomatal conductance and root and shoot characteristics affect crack patterns (Bordoloi et al., 2020). In this paper, the focus will be on the first two points mentioned.

As already mentioned, roots in the soil absorb water and cause an increase in soil suction, reducing its hydraulic conductivity and increasing soil shear strength (Ng and Menzies, 2007; Ng and Leung, 2012). Furthermore, this vegetation-induced suction results in a change in the effective soil stress, which can cause soil shrinkage and initiate the cracking process (Fredlund and Rahardjo, 1993). It has been recognized for years that this root desiccation process can cause damage to shallow foundations and road paving in clayey soils (Croney and Lewis, 1948; Ward, 1948; Parry, 1992).

So, roots have a mechanical effect on the soil, which can increase the apparent soil cohesion, also called root cohesion. The increased amount depends on the density and strength of the roots. These characteristics in turn depend on the age and growth rate of the roots, in addition to the plant species (Genet et al., 2005; Loades et al., 2015; Boldrin et al., 2017). Comparing the roots with natural fibers, it can be stated that due to the increased soil tensile strength by natural fibers, the soil tensile strength increased, the crack resistance of soil is improved, and hence CIF is reduced (Consoli et al., 2011; Tang et al., 2021).

Roots in the soil induce suction, which can decrease permeability, increase soil tensile strength, and accelerate the cracking process. However, considering that roots are natural fibers that increase soil's tensile strength, the crack resistance of the soil increases. It is noted that vegetation has its positive and negative aspects from the point of view of civil engineering (Genet et al., 2005; Boldrin et al., 2017).

In-depth studies of the cracking process were carried out both in the laboratory and in the field. It is important to point out that most of the research was done in the laboratory, allowing greater control of the environment. However, it is precisely this control that can make the research less representative than those carried out in the field (Miller et al., 1998).

It is necessary to have a better understanding of the evaluation of the crack formation and propagation process in soils and evaluate the impact of this phenomenon to understand the mechanical and hydraulic behavior better. This study aimed to demonstrate that the hydro geotechnical behavior, the pattern of the cracking formation, and the crack propagation process in the expansive clayey soil of Paulista - Pernambuco, Brazil depend on vegetation and climate, using a field scale. The one-year period allowed the process to be studied also in the dry and wet seasons.

MATERIALS AND METHODS

The soil texture consists of 280 g kg⁻¹ of sand, 250 g kg⁻¹ of silt, and 470 g kg⁻¹ of clay. The liquidity limit is 76 %, the plasticity limit is 30 %, and the grain density (G) of the soil is equal to 2.674 (Ferreira et al., 2017). The soil has a plasticity index of 46, indicating a soil with very high plasticity, according to Burmister's criteria (1949). The soil originated from the physical-chemical weathering of clay and limestone from the Maria Farinha Formation (Bastos, 1994). The local climate is hot and humid tropical with an accentuated dry period of 7 to 8 months, being classified as As' according to the criteria of Köppen and Geiger. The average annual temperature at the sampling site is 26 °C and the average annual rainfall is 1819 mm. The soil is acidic [pH(H₂O) 4.93], eutrophic (V value = 56.80 %), highly active (T = 40.92 cmol_c kg⁻¹) and has irregular interstratification involving 2:1 minerals with micas and expansive minerals (smectites), as well as kaolinite (Ferreira et al., 2017).

Field test location and execution

Field crack tests were carried out at the Janga Sewage Treatment Station, located in Maranguape II neighborhood, in the city of Paulista - Pernambuco (Latitude: 07.00° 55.00' 35.00" S; Longitude: 34.00° 50.00' 49.00" W, Figure 1).

The climate in the region is hot and humid, according to Köppen classification system (As'). Through the database of the National Institute of Meteorology (INMET) it was possible to access climate data for the region during the period of tests (Figure 2). During this time, total precipitation and evapotranspiration were 1547.63 and 842.67 mm, respectively, while the average temperature was 26.30 °C.

September, October, and November correspond to the dry season, in which evapotranspiration exceeds precipitation, and temperatures are the highest of the year. March, April, May, June, and July correspond to the rainy season, in which rainfall is greater than evapotranspiration and temperatures are lower. Maximum and minimum temperatures correspond to the highest and lowest temperatures of the month, which are averaged.

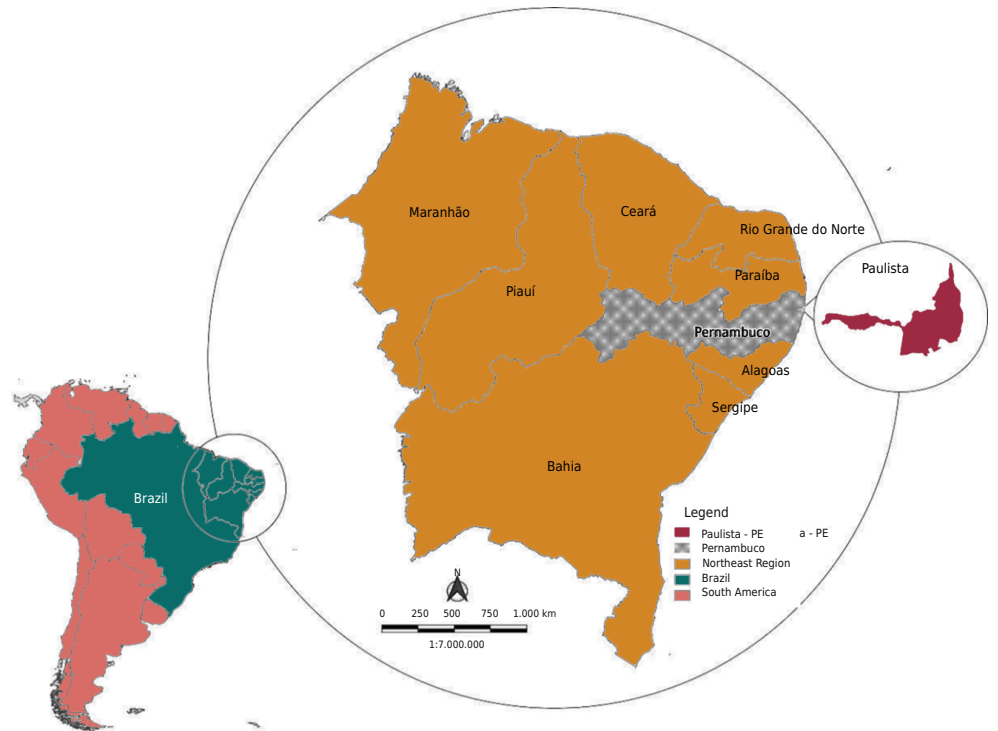


Figure 1. Location of the city of Paulista, Pernambuco.

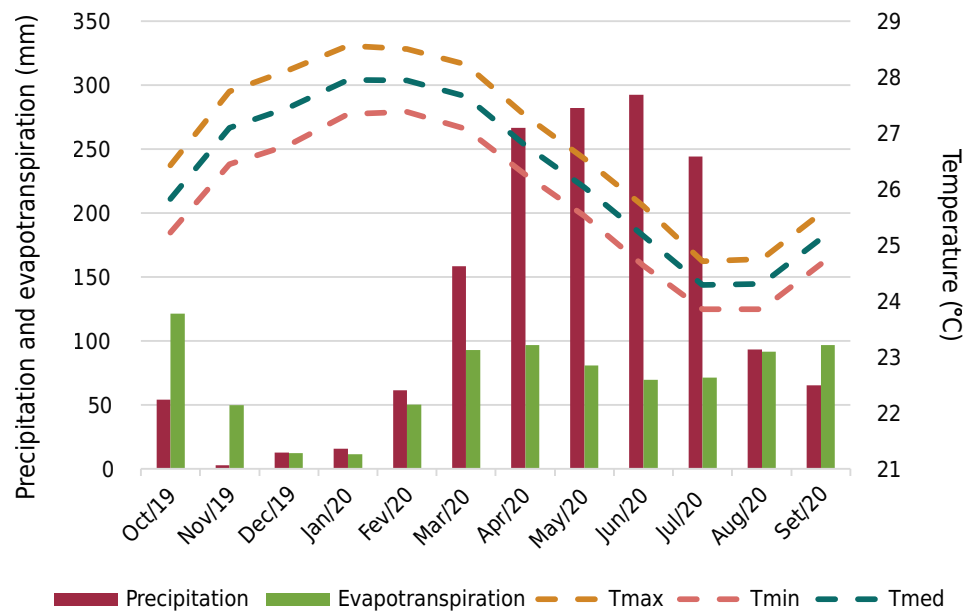


Figure 2. Measurements of precipitation, evapotranspiration, maximum, minimum, and average temperature.

Initially, two study areas were demarcated, both with a square section of 0.60 m on each side, with wooden pickets and plastic ribbon. In the area designated for the study without vegetation, a 0.15 m deep excavation was made to remove the vegetation with its roots and in the end, the surface was leveled. Drainage of this excavation was planned to avoid rainwater accumulation.

Galvanized metal frames were fixed to the ground, and a hollow aluminum plate was welded to the end of the frame to position the camera. Wooden battens 0.20 m long and 0.05 m wide were made. Graph paper was glued to each batten to serve as a reference for the three-dimensional images. Finally, to prevent the site from being trampled on, the studied region was surrounded with nylon mesh. Details of the assembled equipment can be seen in figure 3.

Twelve visits were made to the study site between October/2019 and September/2020 to capture photos for analysis of soil cracks with and without vegetation. Table 1 presents the sequence of visits carried out. On each visit to the study site, the camera was positioned on the hollow aluminum plate to collect the standardized images. Once the image collection stage was completed, a portion of the surface soil was collected to determine the matric suction using the filter paper method and soil moisture. The same procedure was performed for the two regions.

Data analysis

Cracking mechanism along the soil drying process was studied using the public domain computer program called ImageJ. This software processed the photos collected through a webcam or semi-professional camera and several geometric indices were obtained (cracked area, CIF, average crack width, crack total length, and the crack segment number). The procedure for processing images in the program is described by the flowchart in figure 4.

The CIF (Crack Intensity Factor) is obtained by the ratio between the cracked area and the initial area of the sample (Miller et al., 1998). The average width of a crack is calculated as the shortest distance from a point on an edge to the opposite boundary of a crack. The total crack length is calculated by counting the total number of black pixels after the image has been skeletonized, and the number of crack segments is the sum of elements between two adjacent intersections.

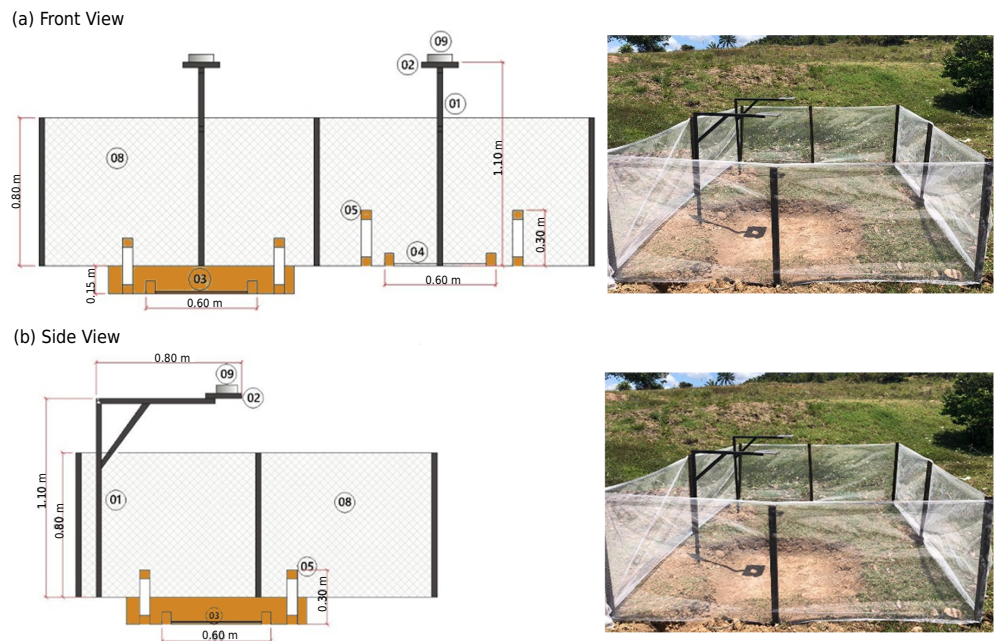
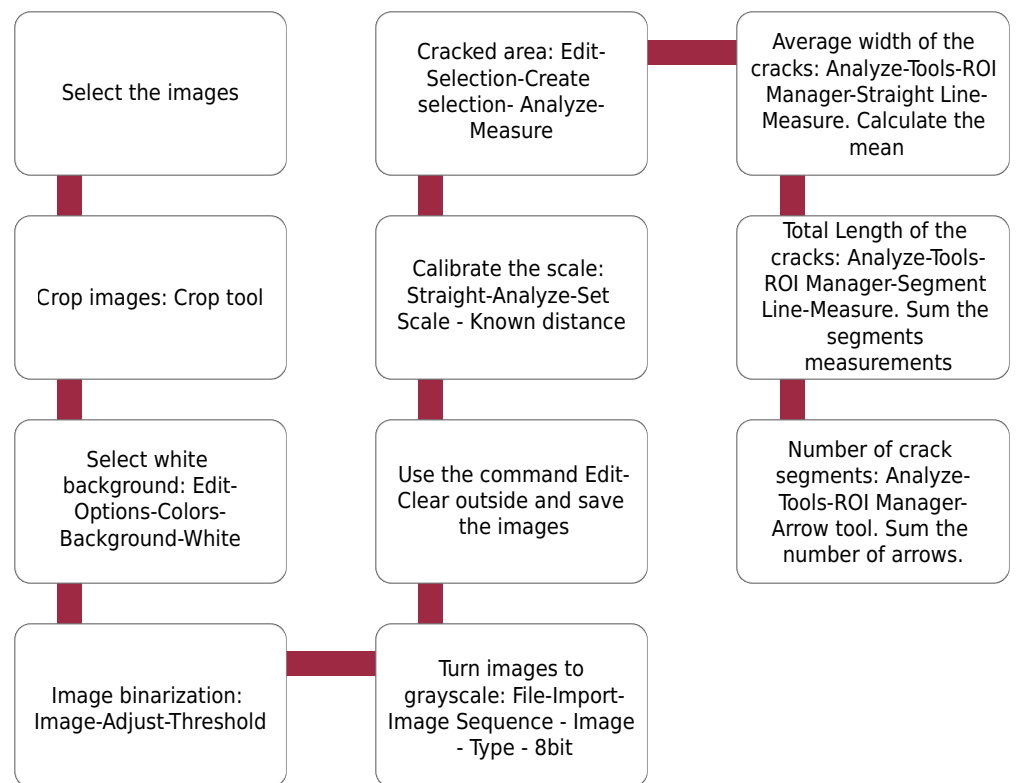


Figure 3. Details of the equipment for analyzing the formation and propagation of cracks in the field: 01 - portico; 02 - support for the camera; 03 - study area without vegetation; 04 - the study area with vegetation; 05 and 06 - references for 3D image analysis; 07 - drainage of the area without vegetation; 08 - protection screen; 09 - photo camera.

Table 1. Soil physicochemical characterization before the beginning of the experiment

Visitation number	Date	Temperature	Relative Humidity - RH
		°C	%
C3	10/17/2019	29.5	75
C4	10/25/2019	30.2	74
C5	11/01/2019	30.1	76
C6	11/07/2019	30.5	74
C7	12/06/2019	30.3	75
C8	12/20/2019	31.4	76
C9	01/29/2020	31.2	77
C10	02/21/2020	31.2	77
C11	03/18/2020	30.1	76
C12	04/01/2020	29.5	79
C13	04/30/2020	28.9	80
C14	09/24/2020	30.1	77


Figure 4. Flowchart for processing images in ImageJ.

RESULTS

The results of the images taken in the field to analyze the formation and propagation of cracks in the soil are presented in a vegetated area and another without vegetation between October/2019 to September/2020. Through the images taken, the crack evolution and geometric indices were evaluated. In total, twelve visits were carried out, and they were named C3 to C14 (Table 1).

Analysis of images of an area without vegetation

The total duration of the study was 342 days or, 8208 h. Initially, the surface moisture of the soil was 15.59 % (C3) without crack. On the second visit (C4), after seven days (168 h), the soil surface already showed the formation of some cracks, and the humidity reduced to 5.71 %. Cracks developed and propagated until the seventh visit (C9), after 104 days (2496 h), with accumulated precipitation of 46.5 mm and surface soil moisture of 5.98 %. The daily precipitation rate from visit C3 to visit C9 was 0.45 mm day⁻¹.

An increase in rainfall was observed from the eighth visit (C10), after 127 days (3048 h), and the natural process of closing the cracks due to soil expansion began. It was verified that all the cracks were closed on the eleventh visit (C13). So, it took 91 days (2184 h) and accumulated precipitation of 522.3 mm, referring to the period between visit C9 and visit C13, corresponding to a daily precipitation rate of 574 mm day⁻¹ and surface soil moisture of 31.91 %. The last visit (C14) was carried out 342 days (8208 h) after the beginning, and despite the soil surface moisture reducing to 15.41 %, no new cracks formed. The accumulated precipitation between visits C13 and C14 was 1070 mm, and the daily precipitation rate was 7.73 mm day⁻¹ (Figure 5). Table 2 presents the summary of the crack analysis results.

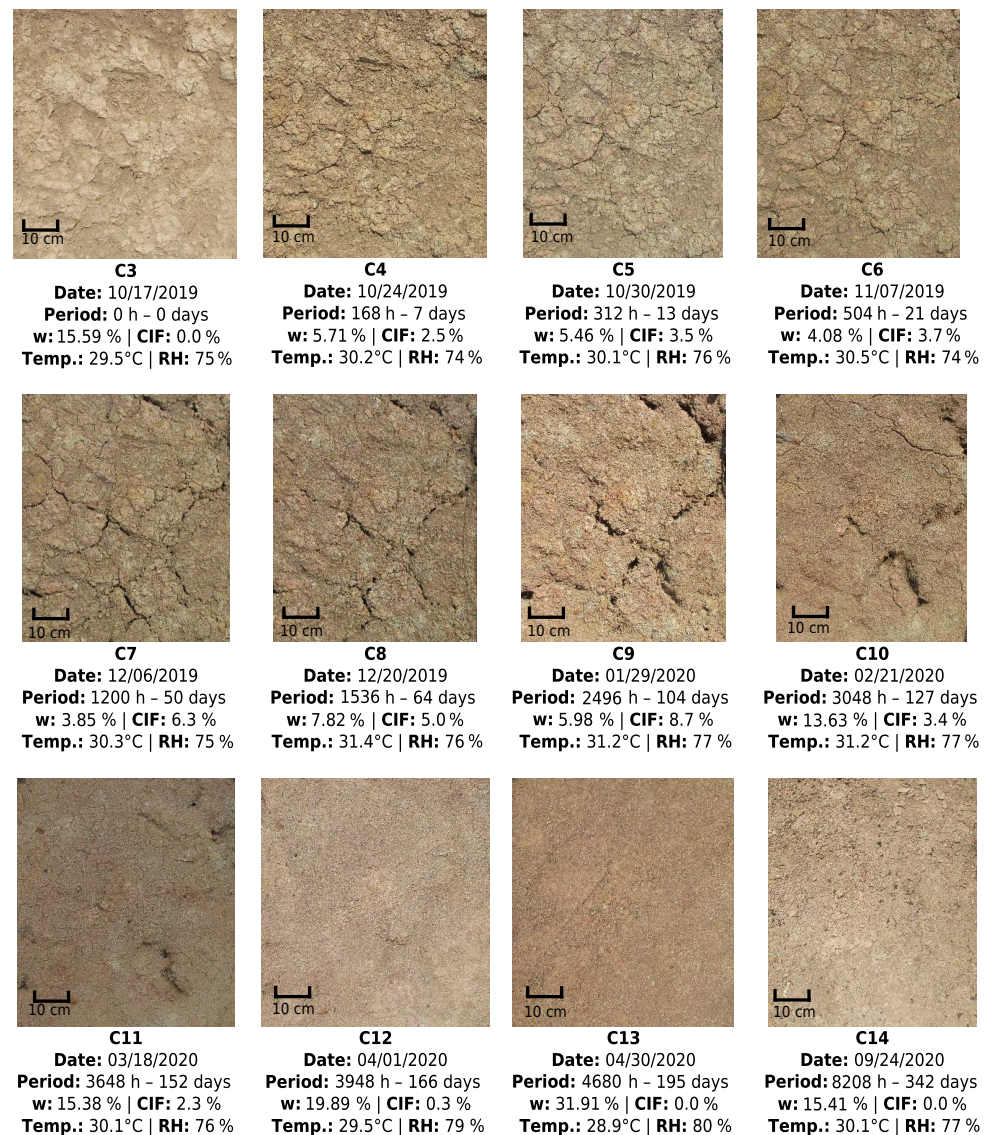


Figure 5. The sequence of images in the area without vegetation.

Table 2. Crack analysis results for the area without vegetation

Visit	Date	Time	Water content	CIF	Medium width	Total length	No. of segment	Temp	Relative Humidity (%)	Matric suction
		h-day	%		mm			°C	%	kPa
C3	10/17/2019	0-0	15.59	0.0	0	0	0	29.5	75	2695
C4	10/24/2019	168-7	5.71	2.5	3.22	717.57	12	30.2	74	33280
C5	10/30/2019	312-13	5.46	3.5	3.33	1478.37	37	30.1	76	33798
C6	11/07/2019	504-21	4.08	3.7	3.37	2262.44	57	30.5	74	36802
C7	12/06/2019	1200-50	3.85	6.3	5.17	4041.9	86	30.3	75	37204
C8	12/20/2019	1536-64	7.82	5.0	5.54	2123.03	62	31.4	76	21543
C9	01/29/2020	2496-104	5.98	8.7	8.75	3049.14	58	31.2	77	3416
C10	02/21/2020	3048-127	13.63	3.4	5.66	2350.69	41	31.2	77	2858
C11	03/18/2020	3648-152	15.38	2.3	4.46	1325.78	28	30.1	76	6502
C12	04/01/2020	3984-166	19.89	0.3	1.26	173.28	7	29.5	79	1050
C13	04/30/2020	4680-195	31.91	0.0	0	0	0	28.9	80	169
C14	09/24/2020	8208-342	15.41	0.0	0	0	0	30.1	77	1985

With these data it is possible to elaborate the curves period versus CIF and water content, period versus temperature and RH, the curves of the quantitative evolution of the geometric cracking indices (cracked area, CIF, average width of cracks, total length of cracks and crack segment number) and the graph period versus daily rainfall during the period of readings in the area without vegetation (Figure 6).

The period versus water content curve (Figure 6a) presents three ranges of water content variation over time. The first range, corresponding to the beginning of the readings (C3) up to 104 days - 2496 h (C9), shows a reduction in soil moisture from 15.59 to 5.98 % in this period and has a range of moisture loss equal to 0.09 %/day. The second range, starting at the end of the first stretch (C9) up to 195 days - 4680 h (C13), shows a gradual increase in soil moisture from 5.98 to 31.91 % over time and a rate of increase of humidity equal to 0.3 %/day. The third and last range begins at the end of the second range (C13) up to 342 days - 8208 h (C14), showing a reduction in soil moisture from 31.91 to 15.41 %, which results in a rate of moisture loss of 0.1 %/day.

There are also three ranges of variation in the Period versus CIF curve (Figure 6a). The first range shows an increase in CIF over time from the start of the trial (C3) to 104 days - 2496 h (C9), with a rate of change in CIF of 0.08 %/day. The second range shows a reduction in the CIF over time due to the increase in rainfall at the research site and comprises between the end of the first range (C9) up to 4680 h - 195 days (C13), with a CIF variation rate equal to at 0.1 %/day. Finally, the third band starts at the end of the second band up to 342 days - 8208 h (C14) and represents the CIF stabilization stage as a function of time.

Average temperature over the readings was 30.3 ± 0.75 °C, with a coefficient of variation equal to 0.02. The mean relative humidity (RH) was 76 ± 1.83 %, with a coefficient of variation of 0.02 (Figure 6b). The variation of geometric indices (cracked area, CIF, average crack width, total crack length and the number of crack segments) as a function of the period (Figure 6c) increased as the soil dried out. With the increase in soil moisture, a decrease in all geometric indices was verified, followed by stabilization. Figure 7 shows the variation of the geometric indices of the cracks during the natural process of drying and wetting the soil. During the drying phase (Figure 7a), there was an increase in all indices with the soil drying. The humidity, when reaching the value of 5 %, presented stabilization, but all geometric indices continued to increase.

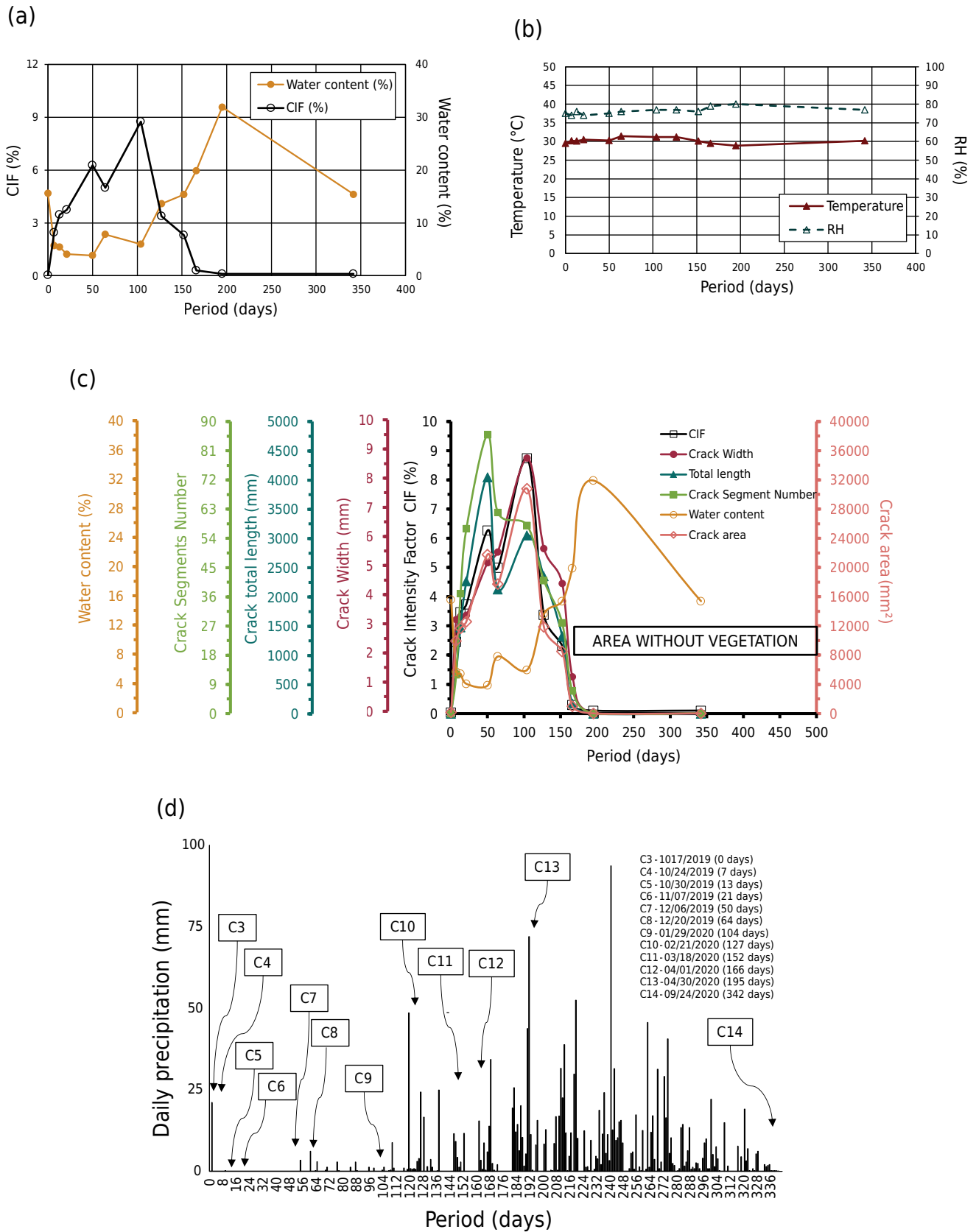


Figure 6. Results for the area without vegetation: (a) period versus water content and CIF; (b) period versus temperature and RH; (c) period versus quantitative evolution of geometric cracking indices (cracked area, CIF, average crack width, total crack length and crack segment number); (d) weather versus daily precipitation during the period of readings.

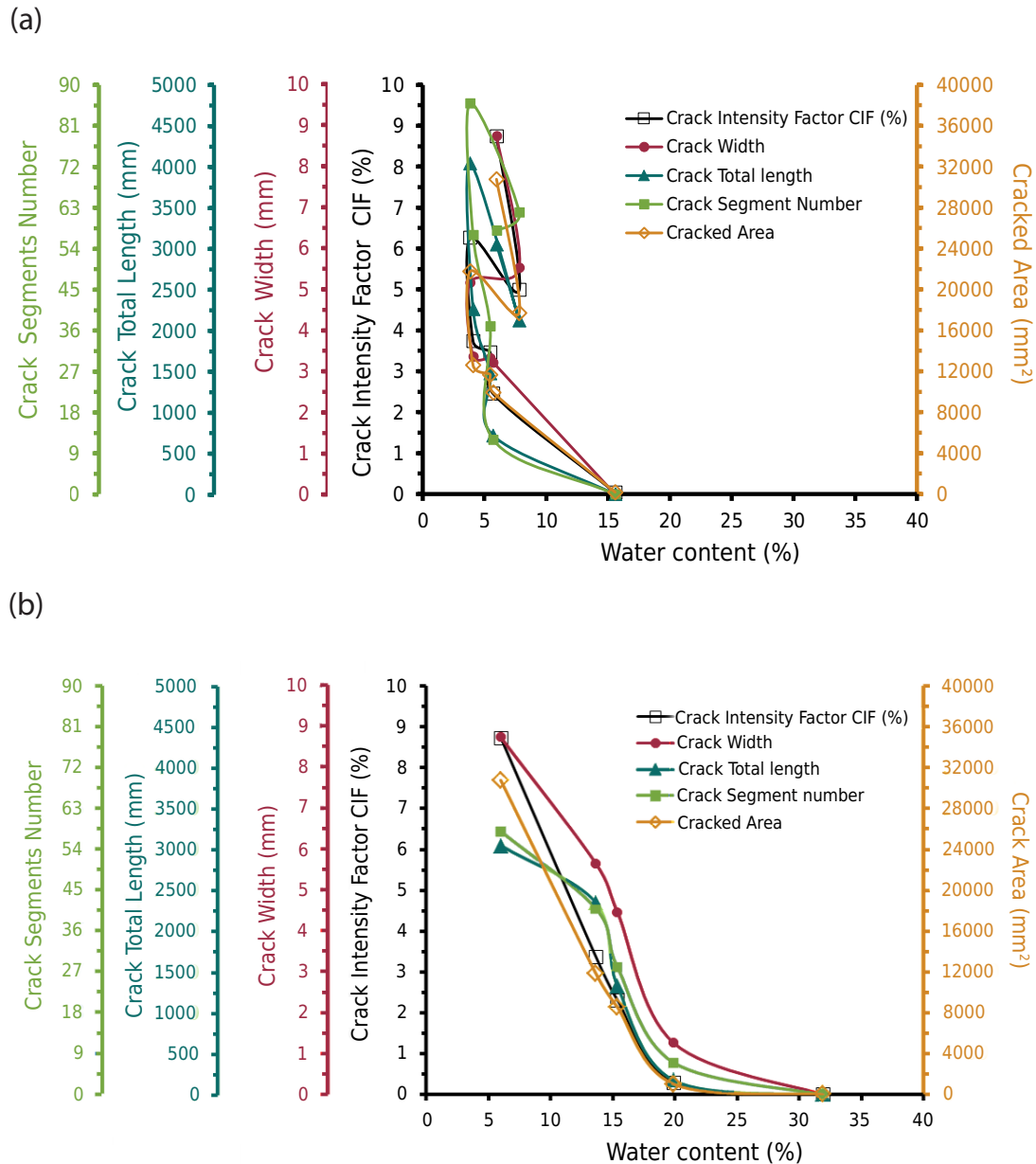


Figure 7. Quantitative evolution of geometric cracking indices in the region without vegetation: (a) drying phase; (b) wetting phase.

Figure 8 presents the soil water retention curve with van Genuchten (1980) adjusted. Table 3 presents the fit indices used in this model. Saturated water content is the saturation moisture at which all the voids in the soil are filled with water. The saturated water content is the saturation moisture content at which all voids in the soil are filled with water. In the first stretch of the retention curve, the soil remains saturated until it reaches the air intake suction. The suction starts to vary when air enters the voids, due to the evaporation of water molecules. Increases in suction greater than air intake will produce appreciable losses in soil water content, reaching a point of change in the slope of the curve, which determines residual moisture. With the drying period, the soil contracts and forms crack.

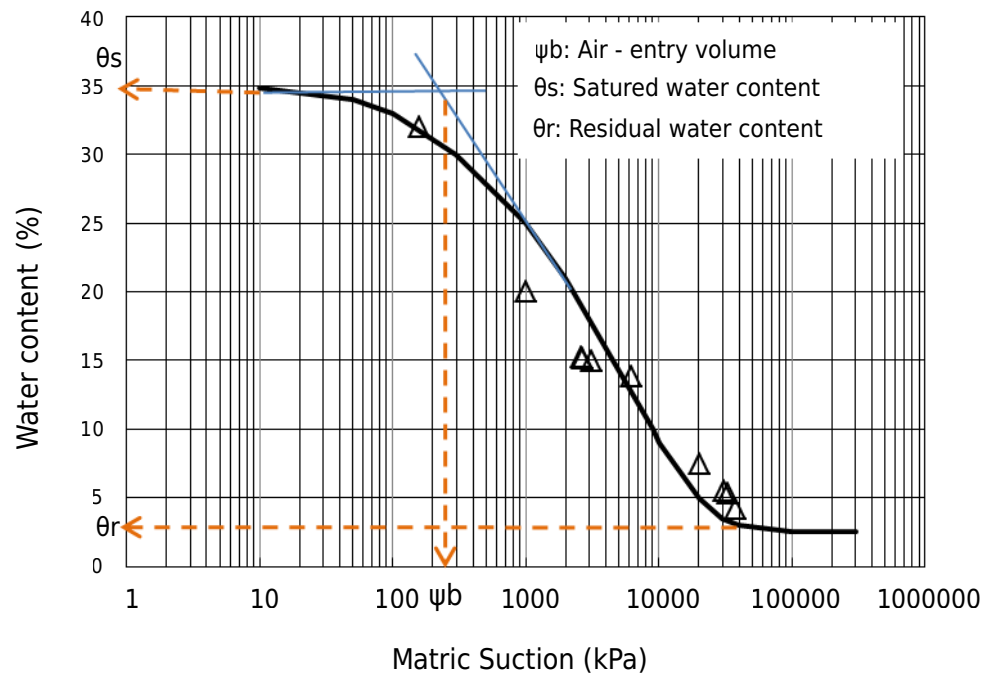


Figure 8. Soil water retention curve from the tests carried out when the image was collected in the area without vegetation.

Table 3. Model fit indices in the area without vegetation

Curve	Residual water content - θ_r	Saturation water content - θ_s	α	n	m	Suction - ψ_b	Differential Moisture Capacity: $C = \Delta_w / \Delta_{\log s}$
	%					kPa	%
W x Sm	3.0	34.5	9.86E-08	0.65	147	250	15

Analysis of images of vegetated area

In the region with vegetation, the crack formation and propagation analysis are carried out, in addition to the percentage evolution of vegetation cover and the variation of water content over time (Figure 9). The total duration of this part of the study was also 195 days (4680 h).

Initially, the soil surface moisture was 4.32 % (C3). Cracking was not noticed until visit C10 ($w = 6.15$ %), after 127 days (3048 h), with accumulated rainfall of 141.1 mm and daily precipitation rate equal to 1.1 mm per day. Cracks developed and propagated only from visit C11 (152 days - 3648 h) to visit C12 (166 days - 3984 h). The accumulated precipitation in this period was 46 mm, and the daily precipitation rate was 3.3 mm per day. Soil moisture between visits C11 to C12 ranged from 6.35 to 10.55 %. The geometric indices (CIF, average width, total length, and number of crack segments) obtained are presented in table 4.

From visit C13 (195 days - 4680 h) until the last reading C14 (342 days - 8208 h), the total closure of cracks was verified, with no new crack formations during this period. The accumulated precipitation in this period was 1078.1 mm, and the daily precipitation rate was 7.3 mm day⁻¹. Soil surface moisture in visits C13 and C14 was 25.28 and 12.21 %, respectively.

Table 5 presents the results of the variation of vegetation in the region. Figure 10 presents the evolution curves of the percentage of vegetation area in the region with vegetation.

The average temperature throughout the readings and average relative humidity (RH) were the same as in the study in the region without vegetation, as the analyses were carried out in parallel on each visit.

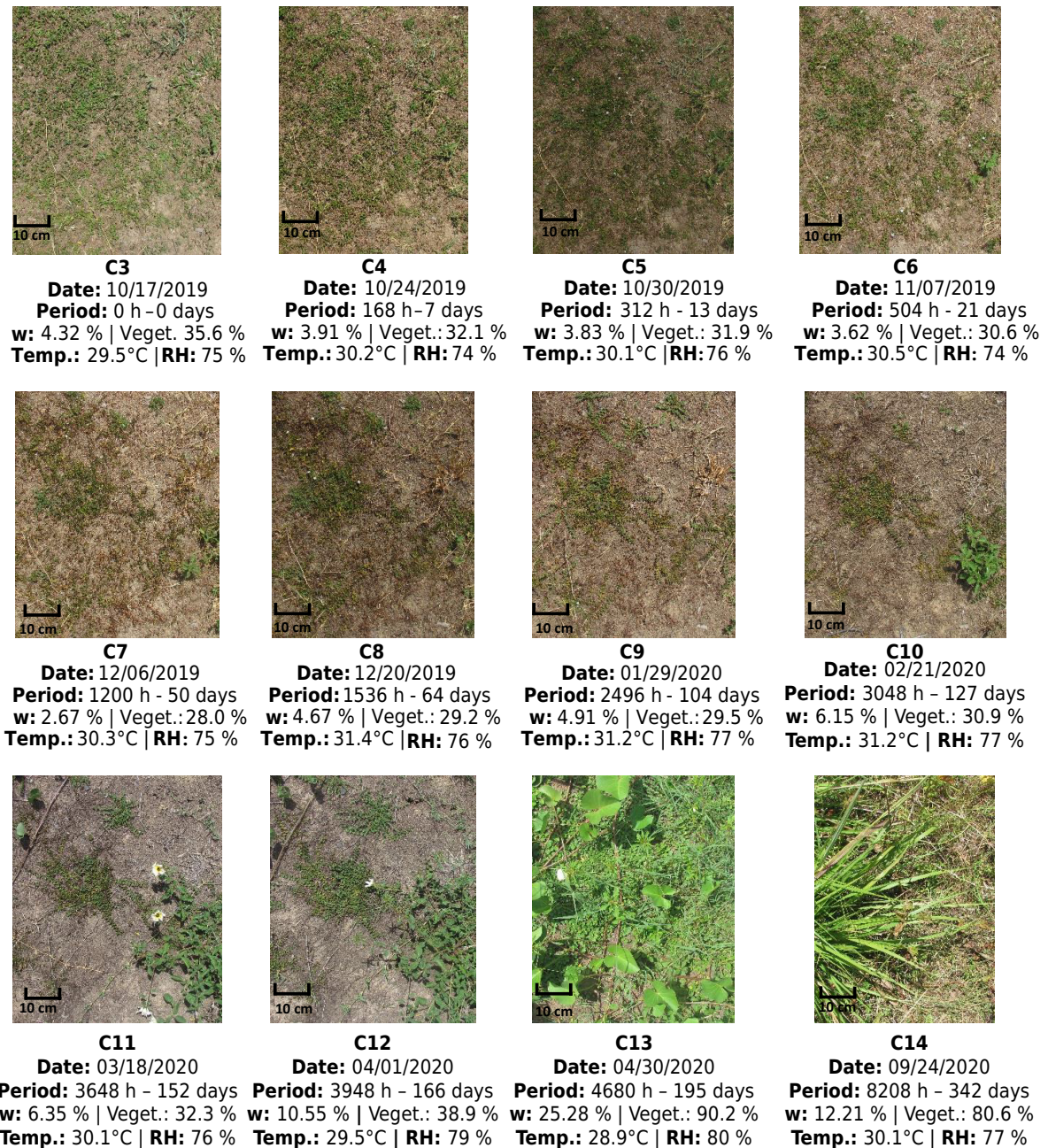


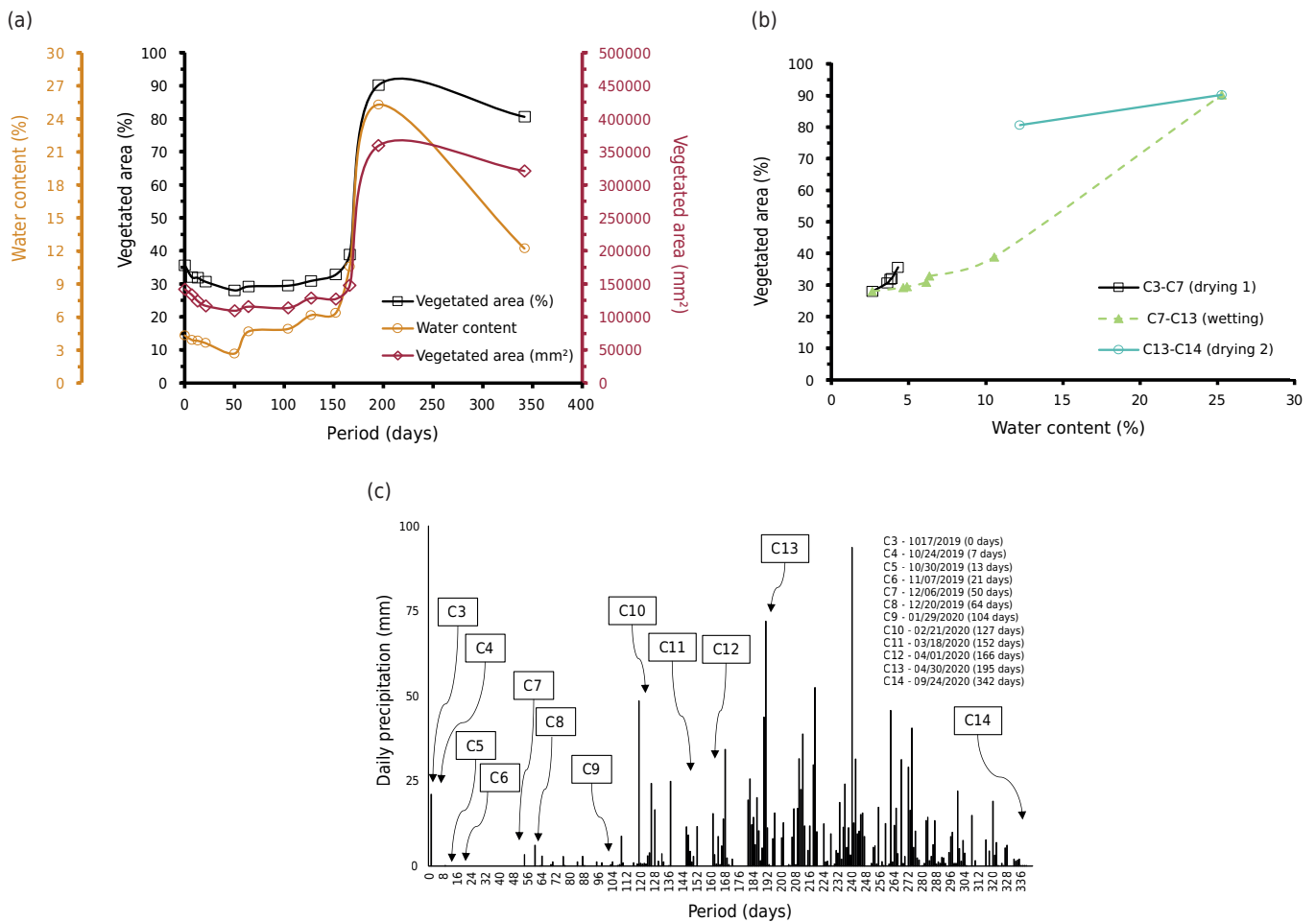
Figure 9. The sequence of images for area with vegetation.

Table 4. Summary of crack analysis results for area with vegetation

Visit	Date	Time	Water content	CIF	Medium width	Total length	No. of segment	Temp	Relative humidit	Matric suction
		h-day	%		mm			°C	%	kPa
C11	03/18//2020	3648-152	6.35	0.3	7.99	174.9	5	30.1	76	6502
C12	04/01/2020	3984-166	10.55	0.9	15.02	182.9	3	29.5	79	1050

Table 5. Crack analysis results for area with vegetation

Visit	Date	Time()	Water content	Vegetated area	Temp	Relative humidit	Matric suction
		h-day	%	%			
C3	10/17/2019	0-0	4.32	35.6	29.5	75	2695
C4	10/24/2019	168-7	3.91	32.1	30.2	74	33280
C5	01/11/2019	312-13	3.83	31.9	30.1	76	33798
C6	11/07/2019	504-21	3.62	30.6	30.5	74	36802
C7	12/06/2019	1200-50	2.67	28.0	30.3	75	37204
C8	12/20/2019	1536-64	4.67	29.2	31.4	76	21543
C9	01/29/2020	2496-104	4.91	29.5	31.2	77	3416
C10	02/21/2020	3048-127	6.15	30.9	31.2	77	2858
C11	03/18//2020	3648-152	6.35	32.8	30.1	76	6502
C12	04/01/2020	3984-166	10.55	38.9	29.5	79	1050
C13	04//30/2020	4680-195	25.28	90.2	28.9	80	169
C14	09/24/2020	8208-342	12.21	80.6	30.1	77	1985


Figure 10. Results for the region with vegetation: (a) Time versus the evolution of the area of vegetation and humidity; (b) weather versus daily precipitation during the period of readings; (c) humidity versus percentage of vegetated area.

As for the vegetation in the area, there were three ranges of variation. The first range lasted from the beginning of the readings (C3) until the C7 visit, with a total duration of 50 days (1200 h), and there was a decrease in the vegetation area from 35.6 to 28.0 % (Figure 10a). During this time, there was a precipitation accumulation of 21.3 mm (Figure 10c), representing a low precipitation index, and a reduction in soil moisture from 4.32 to 2.67 % (Figure 10b), to which justifies the vegetation area reduction in this period. The reduction rate of the vegetation over that period was equal to 0.15% per day.

The second range started after visiting C7 until visit C13, lasting 145 days (3480 h), showing an increase in vegetation area from 28.0 to 90.2 % (Figure 10a). During this period, an accumulation of rainfall of 546.6 mm was recorded (Figure 10c). This represents a significant increase in precipitation, increasing soil moisture from 2.67 to 25.28 % (Figure 10b). The rate of vegetation increase over that period was 0.43% per day.

Finally, the last lane started from visit C13 to visit C14, lasting 147 days (3528 h), showing a reduction in the vegetation area from 90.2 to 80.6 % (Figure 11a). An accumulation of rainfall equal to 1078.1 mm was recorded during this period (Figure 11c). Topsoil moisture decreased from 25.28 to 12.21 % (Figure 10b). The vegetation percentage reduction rate was 0.07% per day. Although this range had the highest accumulation of rainfall, there was a reduction in the vegetation area. This can be explained by the greater rainfall concentration right after the C13 visit, and as visit C14 approached, there was a considerable reduction in rainfall (Figure 10c).

As in the region without vegetation, on each visit to the study site, the matrix suction of the surface soil was determined using the filter paper method. Figure 11 presents the soil water retention curve with van Genuchten (1980) adjusted. Table 6 presents the fit indices used in this model.

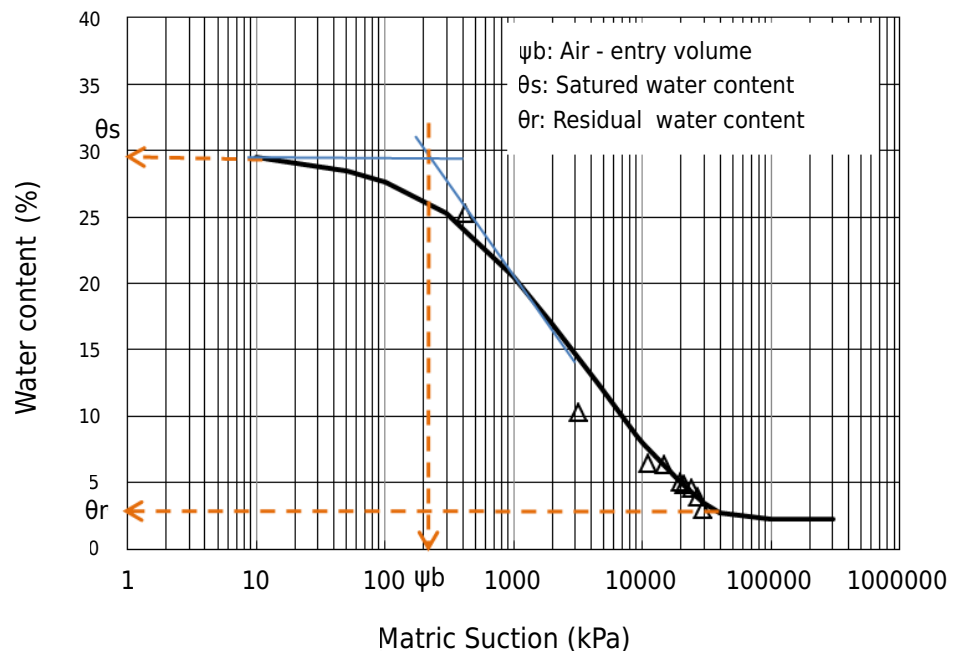
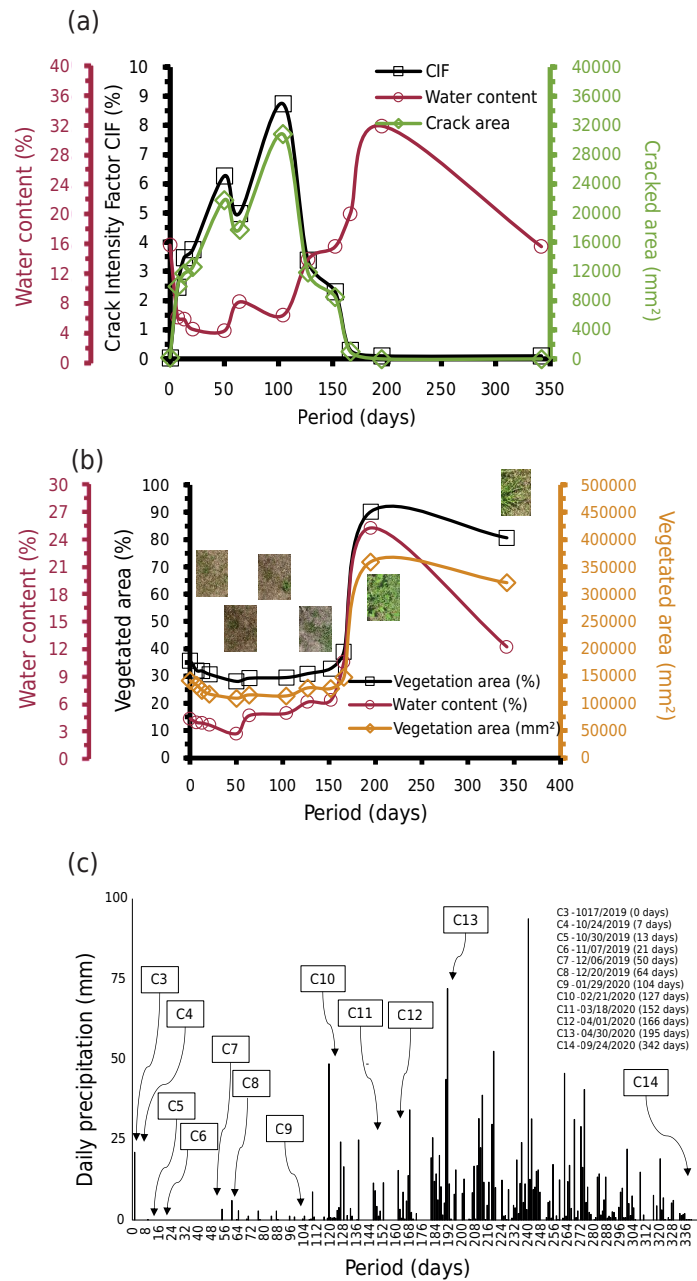


Figure 11. Soil water retention curve from the tests carried out when the image was collected in the area with vegetation.

Table 6. Model fit indices - Area with vegetation

Curve	Residual water content - Θ_r	Saturation water content - Θ_s	α	n	m	Suction - ψ_b	Differential Moisture Capacity: $C = \Delta_w / \Delta_{\log S}$
	%					kPa	%
W x Sm	2.1	29.2	9.86E-08	0.64	135	200	14.5


Figure 12. Effect of climate (rainfall) on: (a) formation of fissures in the region without vegetation; (b) variation of the area of vegetation in the area with vegetation; (c) daily rainfall from 10/17/2019 to 09/24/2020.

Comparison of crack formation and propagation between field tests

Figure 12 shows the effect of climate on the formation of cracks in the region without vegetation and on the variation of the vegetation area in the region. The formation and propagation of cracks in the region without vegetation increased during the dry season. With the onset of rains, the cracks then closed completely and remained so despite the reduction in soil surface moisture, as desiccation was not sufficient to reopen pre-existing cracks or form secondary cracks (Figure 12a).

During the dry season, the vegetation area remained constant in the area with vegetation, at approximately 30 %. With the increase in rainfall, the surface soil increased moisture, and therefore, there was an increase in vegetation area, reaching approximately 90 % of the area with vegetation. With the end of the rainy season, soil moisture decreased, and there was a reduction in the vegetation area (Figure 12b). Figure 13 shows the evolution of crack formation and propagation as a function of time in regions with and without vegetation.

The initial soil moisture in the region with vegetation was equal to 4.32 % and did not show surface cracks. In the region without vegetation, the initial soil moisture was equal to 15.59 %. The topsoil in this region was confined to 0.15 m below the ground surface due to the removal of vegetation and roots at the beginning of the study. Therefore, the initial humidity of the surface soil in the region without vegetation was higher.

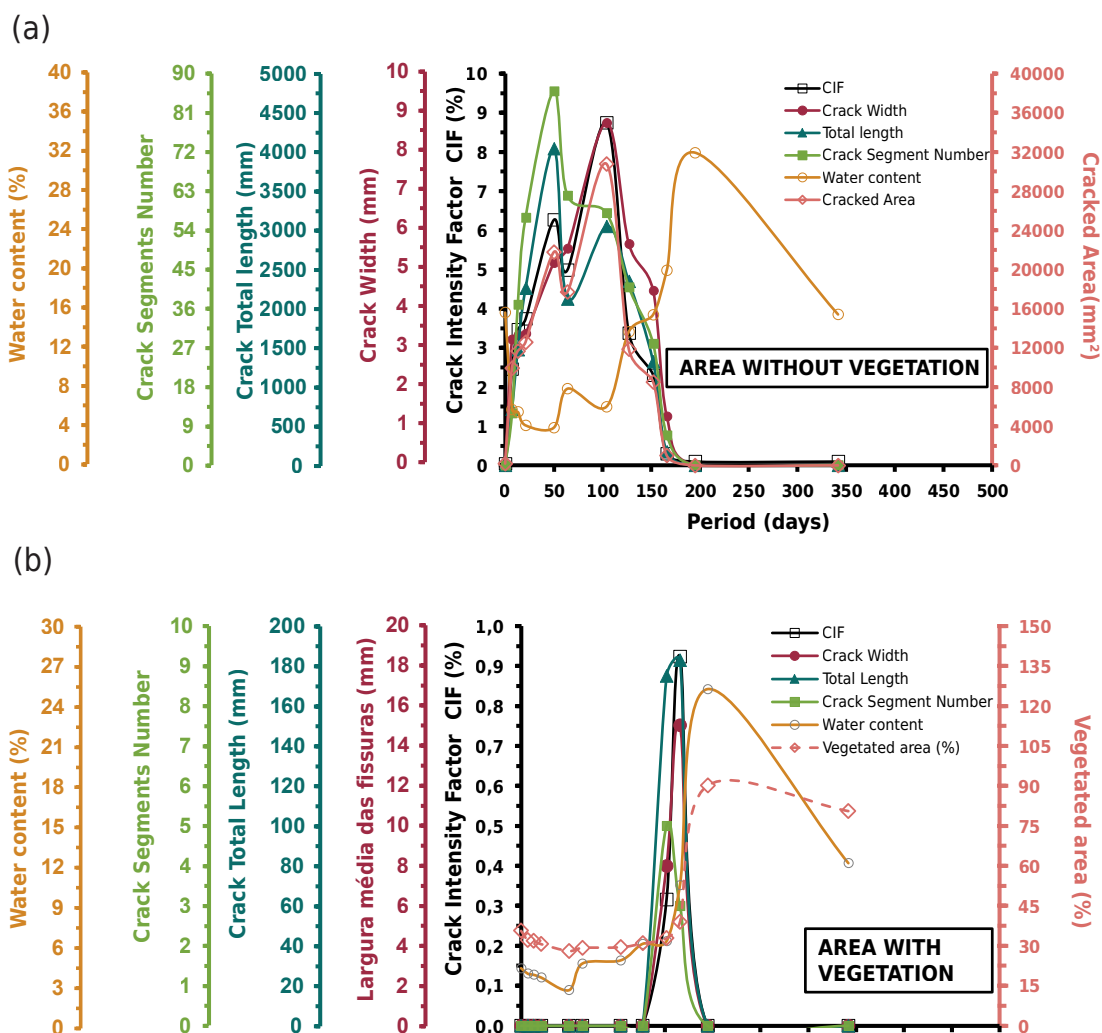


Figure 13. Period versus Geometric evolution of cracks: (a) area without vegetation; (b) area with vegetation.

With the open-air soil exposure in the region without vegetation, there was a decrease in humidity and the geometric indices increased up to approximately 100 days from the beginning of the readings. Later, with the increase in rainfall in the area, the humidity increased, and the soil expanded. Consequently, a reduction in the geometric indices of the cracks was verified. After 180 days from the readings' beginning, the cracks' complete closure was verified, with surface soil moisture equaling 31.91 %. Then, with the decrease in rainfall, the surface soil moisture again reduced to 15.41 % after 342 days after the beginning of the readings, and there was no formation of new cracks.

In the region with vegetation, no formation of cracks was observed up to 140 days after the beginning of the readings. During this period, soil moisture showed low values (2.67 to 6.15 %). A few cracks were formed 140 days after the beginning of the readings, and the geometric indices increased. Approximately 200 days after the beginning of the readings, the cracks closed, that is, the geometric indices became null again.

DISCUSSION

Area without vegetation

In the area without vegetation, it was noticed that there was soil desiccation with the dry season, and cracks were formed (increase in CIF). As rainfall increased at the site, soil moisture increased, causing expansion and, therefore, a decrease in the cracked area of the soil until stabilization, with zero CIF. The same phenomenon was observed by Ribeiro Filho et al. (2023).

The soil had a water content of 15.59 % (initial drought), there was a decrease in water content due to evaporation, and the geometric indices increased up to approximately 100 days from the beginning of monitoring, with surface soil moisture equal to 5.98 %. In the rainy season, water content increased, the soil expanded, and cracks decreased. There was a reduction in the crack geometric indices, and after 180 days from the beginning of the monitoring, the surface cracks were closed, with surface water content equal to 31.91 %. With the decrease in rainfall, the surface soil moisture reduced to 15.41 % after 342 days from the beginning of the readings, with no formation of new cracks.

The average width of the cracks increased from the beginning of the test (C3) to 104 days - 2496 h (C9), with a variation rate equal to 0.08 mm per day. With increasing soil moisture, there was a reduction in the average width of the cracks during the C9 visit period up to 195 days - 4681 h (C13), with a variation rate of the average width of the cracks equal to 0.1 mm per day. Between visits C13 and C14, the average width of the cracks stabilized. The total length and number of crack segments increased from the beginning of the test (C3) to 50 days - 1200 h (C7), with a variation rate equal to 80.8 mm per day and 1.7 units per day, respectively. With increasing soil moisture, there was a reduction in the total length and number of crack segments during the C7 visit up to 195 days - 4680 h (C13), with a variation rate equal to 27.9 mm per day and 0.6 units per day, respectively. Between visits C13 and C14, both indices stabilized.

The geometric indices (CIF, average width, total length, and segment number) increase with drying. No stabilization of the geometric indices was verified. The indices continued increasing with soil water content stabilization. This is because soil water content was obtained at the surface. Probably, below the surface, soil water content was higher due to confinement. With the advance of soil cracking in-depth, they also began to dry out with the opening of the crack, and thus, these layers began to dry out, and the geometric indices continued to increase. That is, the geometric indices continued increasing as the layer below the surface continued to lose water with desiccation, even with the stabilization of topsoil water content. As for the shape of the cracks developed, it is

observed that the secondary cracks were formed from the primary cracks, presenting "T" and "X" shapes (Figure 6).

With the increase in rainfall, the wetting phase began (Figure 8b). With wetting, the soil expanded, and all geometric indices decreased until the complete closure of the cracks, that is, stabilization occurred with zero value of the geometric indices. In other studies, carried out in semi-arid regions, this correlation between rainfall and evolution or stabilization of geometric indices was also noted (Ribeiro Filho et al., 2023). Correlating the intensity of cracking with the clayey fraction of the soil (Elias et al., 2021; Ribeiro Filho et al., 2023), it is noted that there is a large cracking in the non-vegetated area, also because the clayey soil studied.

Vegetated area

In the experimental area with vegetation, the formation of cracks was not verified until 140 days from the beginning of the monitoring, in the dry period. A few cracks were formed 140 days after the readings began, and the geometric indices increased. After 200 days from the reading's beginning, in the rainy season, the cracks closed, and the crack geometric indices became null again.

The vegetated area presented small number of primary cracks, absence of secondary, and its shape was linear. The few cracks that existed were not formed when soil moisture was lower, but after the increase in rainfall in the region. This late crack propagation, when compared to the area without vegetation, can be explained by the influence of vegetation on the soil, increasing the surface traction resistance of the soil by the roots during the desiccation period.

It can be concluded that in the dry season, there was a reduction in the vegetation area. As there was an increase in rainfall at the site, soil moisture increased, and thus, the vegetation area increased. It was also verified by Silva (2001) that, during the summer months, when rainfall is scarce, temperature and insolation are high, vegetation practically disappears, and cracks appear in the most superficial soil layers.

It is noteworthy that, in the region with vegetation, a few cracks were formed in a period in which the humidity of the surface soil increased (increase in rainfall). However, with the continuous increase in rainfall and, consequently, in soil moisture and the percentage of vegetation, the cracks closed.

Thus, the surface soil water content in the experimental area with vegetation is lower than without vegetation (except in a determination in the rainy season). The values of residual water content, saturation water content, and differential moisture capacity in the soil area without vegetation (Table 3) are higher than the corresponding values of the area with vegetation (Table 6). This is due to evapotranspiration in the area with vegetation, as opposed to the area without vegetation, where there is only evaporation. It is important to note that even with higher suction in the vegetated area, the crack formation and propagation were smaller because the roots of the vegetation absorb the surface tensions generated by the suction that would be transmitted to the soil if it were not covered with vegetation. The vegetation's importance in minimizing or preventing soil crack formation and propagation was reaffirmed.

According to Elias et al. (2021), the presence of roots in the soil, noted during the study, tend to make the soil drier due to moisture absorption. However, the presence of roots also restricts soil movement in the driest period.

CONCLUSIONS

Vegetation cover has a significant influence on the process of formation and propagation of cracks in the field and in the cracking pattern. Soil moisture in the area with vegetation is lower than in the non-vegetated area due to evapotranspiration occurring in one, while the other only evaporation occurs. During the entire observation period in the field, including the rainy and dry season, in the area with vegetation, practically the appearance of cracks was small. The root of vegetation involved in the soil mass absorbed the tensile stresses imposed by the increase in suction. In the dry period, with the reduction of water in the soil, there is a reduction in the covered area vegetation, and in the area without vegetation cover, the intensity of cracks grows. In the period of the year with higher rainfall intensities, in the area without vegetation, the superficial fissures are closed due to soil expansion and leaching of surface fines into the cracks, and, in the area with vegetation, there is an increase in the intensity of vegetation.

ACKNOWLEDGMENTS

This study was supported by CNPq – Conselho Nacional de Desenvolvimento Científico e Tecnológico, Brazil [grant number 421087/2018-8] and by Coordenação de Aperfeiçoamento de Pessoal de Nível Superior – Brasil (CAPES).

AUTHOR CONTRIBUTIONS

Conceptualization:  Arthur Gomes Dantas Araújo (equal) and  Silvio Romero de Melo Ferreira (equal).

Data curation:  Arthur Gomes Dantas Araújo (equal) and  Silvio Romero de Melo Ferreira (equal).

Formal analysis:  Arthur Gomes Dantas Araújo (equal) and  Silvio Romero de Melo Ferreira (equal).

Funding acquisition:  Silvio Romero de Melo Ferreira (lead).

Investigation:  Arthur Gomes Dantas Araújo (equal),  Martha Maria Bezerra Santos (equal) and  Silvio Romero de Melo Ferreira (equal).

Methodology:  Arthur Gomes Dantas Araújo (equal),  Martha Maria Bezerra Santos (equal) and  Silvio Romero de Melo Ferreira (equal).

Project administration:  Silvio Romero de Melo Ferreira (lead).

Resources:  Arthur Gomes Dantas Araújo (equal) and  Silvio Romero de Melo Ferreira (equal).

Supervision:  Arthur Gomes Dantas Araújo (equal) and  Silvio Romero de Melo Ferreira (equal).

Visualization:  Arthur Gomes Dantas Araújo (equal),  Martha Maria Bezerra Santos (equal) and  Silvio Romero de Melo Ferreira (equal).

Writing - original draft:  Arthur Gomes Dantas Araújo (equal),  Martha Maria Bezerra Santos (equal) and  Silvio Romero de Melo Ferreira (equal).

Writing - review & editing:  Martha Maria Bezerra Santos (equal) and  Silvio Romero de Melo Ferreira (equal).

REFERENCES

- Bastos EG. Volumetric variation of an expansive clay from the north coast of Pernambuco [dissertation]. Campina Grande: Universidade Federal da Paraíba; 1994.
- Boldrin D, Leung AK, Bengough AG. Correlating hydrologic reinforcement of vegetated soil with plant traits during establishment of woody perennials. *Plant Soil*. 2017;416:437-51. <https://doi.org/10.1007/s11104-017-3211-3>
- Bordoloi S, Ni J, Ng CWW. Soil desiccation cracking and its characterization in vegetated soil: A perspective review. *Sci Total Environ*. 2020;729:138760. <https://doi.org/10.1016/j.scitotenv.2020.138760>
- Burmister DM. Principles and techniques of soil identification. In: Proceedings of annual highway research board meeting. Washington, DC: National Research Council; 1949. v. 29. p. 402-34.
- Chen FH. Foundations on expansive soils. New York: Elsevier Scientific Publishing; 1988.
- Consoli NC, Moares RR, Festugato L. Split tensile strength of monofilament polypropylene fiber-reinforced cemented sandy soils. *Geosynth Int*. 2011;18:57-62. <https://doi.org/10.1680/gein.2011.18.2.57>
- Cronev D, Lewis WA. The effect of vegetation on the settlement of roads. In: Biology and civil engineering Conference. London: Thomas Telford Publishing; 1948. p. 195-222.
- Elias EA, Salih AA, Alaily F. Cracking patterns in the Vertisols of the Sudan Gezira at the end of dry season. *Int. Agrophys*. 2021;15:151-5.
- Ferreira SRM, Araújo ADD, Barbosa FAS, Silva TCR, Bezerra IMDL. Analysis of changes in volume and propagation of in expansive soil due to changes in water content. *Rev Bras Cienc Solo*. 2020;44:e0190169. <https://doi.org/10.36783/18069657rbcs20190169>
- Ferreira SRM, Ferreira MGVX. Mudanças de volume devido a variação de teor de umidade em um Vertissolo no semiárido de Pernambuco. *Rev Bras Cienc Solo*. 2009;33:779-91. <https://doi.org/10.1590/S0100-06832009000400004>
- Ferreira SRM, Paiva SC, Morais JJO, Viana RB. Avaliação da expansão de um solo do município de Paulista-PE melhorado com cal. *Rev Matéria*. 2017;22:e11930. <https://doi.org/10.1590/S1517-707620170005.0266>
- Ferreira SRM. Collapse and expansion of unsaturated soils due to flooding [thesis]. Rio de Janeiro: Universidade Federal do Rio de Janeiro; 1995.
- Fredlund DG, Rahardjo H. Soil mechanics for unsaturated soils. New York: John Wiley and Sons; 1993.
- Genet M, Stokes A, Salin F, Mickovski SB, Fourcaud T, Dumail J, Beek RV. The influence of cellulose content on tensile strength in tree roots. *Plant Soil*. 2005;278:1-9. <https://doi.org/10.1007/s11104-005-8768-6>
- Guerreiro MS, Andrade EM, Palácio, HADQ, Brasil JB, Ribeiro Filho JCR. Enhancing ecosystem services to minimize impact of climate variability in a dry tropical forest with Vertisols. *Hydrology*. 2021;8:46. <https://doi.org/10.3390/hydrology8010046>
- Guerreiro MS, Andrade EM, Sousa MMM, Brasil JB, Ribeiro Filho JCR, Palácio HAQ. Contribution of non-rainfall water input to surface soil moisture in a tropical dry forest. *Hydrology*. 2022;9:102. <https://doi.org/10.3390/hydrology9060102>

- Jotisankasa A, Sirirattanachat T. Effects of grass roots on soil-water retention curve and permeability function. *Can Geotech J.* 2017;54:1612-22. <https://doi.org/10.1139/cgj-2016-0281>
- Loades KW, Bengough AG, Bransby MF, Hallet PD. Effect of root age on the biomechanics of seminal and nodal roots of barley (*Hordeum vulgare* L.) in contrasting soil environments. *Plant Soil.* 2015;395:253-61. <https://doi.org/10.1007/s11104-015-2560-z>
- Miller CJ, Mi H, Yesiller N. Experimental analysis of desiccation crack propagation in clay liners. *J Am Water Resour As.* 1998;34:677-86. <https://doi.org/10.1111/j.1752-1688.1998.tb00964.x>
- Nelson JD, Chao KC, Overton DD, Nelson EJ. *Foundation engineering for expansive soils.* New York: Wiley Press; 2015. <https://doi.org/10.1002/9781118996096>
- Ng CWW, Leung AK. Measurements of drying and wetting permeability functions using a new stress-controllable soil column. *J Geotech Geoenviron Eng.* 2012;138:56-68. [https://doi.org/10.1061/\(ASCE\)GT.1943-5606.0000560](https://doi.org/10.1061/(ASCE)GT.1943-5606.0000560)
- Ng CWW, Menzies B. *Unsaturated soil mechanics and engineering.* New York: Taylor & Francis; 2007.
- Parry RH. Desiccation, some examples measured in London clay. In: 7th International Conference on Expansive Soils; August 1992; Dallas, Texas. Lubbock: Texas Tech University; 1992. p. 404-8.
- Ribeiro Filho JC, Andrade EM, Guerreiro MS, Palácio HQ, Brasil JB. Soil-water-atmosphere effects on soil crack characteristics under field conditions in a semiarid climate. *Hydrology.* 2023;10:83. <https://doi.org/10.3390/hydrology10040083>
- Silva JM. *Variação volumétrica de uma argila expansiva não-saturada submetida a diferentes condições climáticas [thesis].* São Paulo: Escola Politécnica da Universidade de São Paulo; 2001.
- Tang C, Zhu C, Cheng Q, Zeng H, Xu J, Tian B, Shi B. Desiccation cracking of soils: A review of investigation approaches, underlying mechanisms, and influencing factors. *Earth-Sci Rev.* 2021;216:e103586. <https://doi.org/10.1016/j.earscirev.2021.103586>
- van Genuchten MT. A closed-form equation for predicting the hydraulic conductivity of unsaturated soils. *Soil Sci Soc Am J.* 1980;44:892-8. <https://doi.org/10.2136/sssaj1980.03615995004400050002x>
- Ward WH. The effect of vegetation on the settlement of structures. In: *Biology and civil engineering Conference.* London: Thomas Telford Publishing; 1948. p. 181-94.